Density Current Simulations In Cold Fresh Water And Its Cabbeling phenomenon: A Comparative Analysis With Given Experimental Results.

Abstract

The behaviour of warm water discharge at a temperature T_m horizontally into a homogeneous body of cold fresh water at a temperature $T = 0$ was investigated by means of a numerical model through lock-exchange. Water density here was taken to be a quadratic function of temperature. Cabbeling process was key as whenever fluid of different temperature come in contact and as well as the development of Kelvin-Helmholtz instability in the interaction surface. Three phases of flow regime was observed as also described by other researchers. The behaviours as described here shows some similarities to those by Nogueira et al. [4], Adduce et al. [9] and Bukreev [13]. We were able to observe in the slumping phase that the collapsing velocity of the denser fluid within this time frame is high, higher than every fluid movement elsewhere. A vigorous mixing was also observed immediately after the collapsing phase that led to a rapid depletion of temperature resulting to a very slow movement of denser fluid. Our result also shows a stepwise movement which might be as a result of the raging columns of the Kelvin-Helmholtz instabilities that causes a partition in the density current. Relations that describes the various regimes $U_{dc}$of flows were also drawn, and as well as those that describes the spreading distance L_{dc} of the density current. But then, there are little variations in the scaling laws as compared to those by Nogueira et al. [4] and Huppert & Simpson [12]. This might be as a result of the fact that the present investigation had considered density variation as a result of temperature difference, with the assumption that density was taken as a quadratic function of temperature. While theirs was by adding salt to the fluid on either side of the barrier experimentally. Density current cases are practical cases that are evident in our nature and human interventions. This work as presented here is practical and relevant to many fields of study and also enhances policy making towards the protection of the aquatic ecosystems as also stated in our previous publication [2].

Keywords: Density current, Cabbeling, Temperature of maximum density.

1 Introduction

Density currents are a phenomenal behaviours that occur in many practical applications both in nature and man-made situations, and examples of such scenarios are given in [1, 2, 3] . Researchers have also extensively studied these behaviours experimentally, theoretically and numerically and have given some mathematical relations and values that describes the propagation speed and spreading distance of such currents and as well as identifying different regimes of flow [2, 4, 5]. However, earlier works on density currents can be found in [6, 7, 8]. Where a much simplified theoretical model that describes the evolution of the frontal head after the release of a denser fluid into a lighter ambient fluid was suggested. A derivation of theoretical model for the initiation of a steady two-dimensional density current in a rectangular channel, and numerical solutions by using the shallow-water equation for a two-layer fluid that has to do with an empirical front condition were also obtained. In practical sense, density currents are bound to occur when two fluids of different densities come in contact or when fluid that is denser is introduced into an ambient fluid which is considered to be less dense. In most of the configurations, the lock-exchange method is used Fig. 1: as this enables such flow scenarios over the rough and smooth horizontal surfaces. Example of such studies with this lock-exchange configuration include [4, 5, 9, 10, 11]. In the case where water masses are on either side of the temperature of maximum density (T_m) come in contact by the instantaneous removal of the gate (lock-exchange), cabbeling is likely to occur even as the various fluids advance in their opposite directions. It is believed that the denser fluid will penetrate the ambient fluid on the floor and form a density current. We can rely on our previous publication [2] for a more detailed literature review in other to minimise repetition.

In that work, we have considered a "Numerical Simulations of the Cabbeling phenomenon in Surface Gravity Currents in Cold Fresh Water" where we have extensively discussed the behaviour of such flows taken density as a quadratic function of temperature. Relations were also drawn that describes the propagation speed of the frontal head and as well as the distance traveled with respect to time [2]. The behaviour of the negatively buoyant plume as mixed fluid that have mixed up to the T_m was also key. But then, behaviour of the descended fluid on the floor was not fully captured and as such, the propagation speed of the density current was not detailed. Though, this might be as a result of the limited domain space. Thus, taken into consideration here is the motion of fluids with T_m (which is $3.98^{\circ}C$ for fresh water at atmospheric pressure, (i.e., approximately $4^{\circ}C$ in some numerical calculation)) initially at rest but separated by a vertical barrier in a rectangular domain with an ambient fluid with temperature zero. It is expected that difference in the hydrostatic pressure will result in the denser fluid flowing in one direction along the floor once the barrier is lifted up. Meanwhile the less dense fluid will flow in the opposite direction horizontally along the upper part of the domain, and this in turn create a mixing layer between the two fluids as they interact with each other. However, the interaction process will continue even as the most dense fluid is located at the lower part with a frontal or leading head until the dense but warm fluid will mix to a point where it becomes the same temperature with the ambient fluid.

We have also observed in most of the earlier experimentally studied cases that the initial density difference is usually by adding salt to the fluid on either side of the barrier, so as to produce a denser fluid [5, 11, 12]. Meanwhile, there are few works that have considered density current flows where density variation is as a result of temperature difference [2, 13]. However, they have not presented a detailed description of the evolution of the frontal head and as well as obtaining some empirical scaling laws that will describe the propagation speed and spread length of the density current. Our present investigation is based on numerical simulations that uses the lock exchange method with the assumption that density is a quadratic function of temperature. Density current which contains a dense but warm fluid in this case is expected to mix further as it spreads outward on the floor. This will continue until the dense fluid will mix to a point where it becomes the same temperature with the ambient fluid. Though, this will be feasible if the domain of computation is extremely large or infinite.

We will vary computational domain between length $L = 7000$, i.e., $0 \leq X \leq 7000$, with a domain height $H = 1000$ i.e., $0 \leq Y \leq 1000$ in the first instance with barrier position $L/14$. And a computational domain

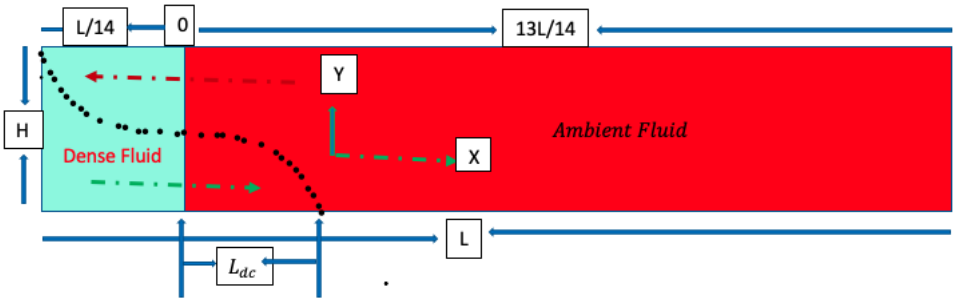

Fig. 1: Schematic presentation of Lock-exchange flow in a channel of length L and height H. The dotted line gives the interface between the two fluids some time after the release.

length $L = 10000$, i.e., $0 \leq X \leq 10000$, with a domain height $H = 1200$ i.e., $0 \leq Y \leq 1200$ in the second instance with barrier position $0.07L/14$. The input fluid temperature in both cases is $\phi_{in} = 1$ on the right hand side. Meanwhile, on the left hand side, at position $13L/14$ and $13.93L/14$, $\phi_{in} = 0$. Where L is the total length of the computational domain and ϕ_{in}, the initial temperature on the various sides of the barrier. Now, reason for the various computational domain is to enable us capture important features and processes for detailed analysis.

2 Model Formulation and Governing Equations

The behaviour of density currents as denser fluid spread outwards on the floor after the lock release due to the nonlinear relation between density ρ and temperature T is very paramount. Thus, the relation below is useful for this study,

$$\rho = \rho_m - \beta(T - T_m)^2 \tag{1}$$

This, we believe gives a very good fit to the experimentally determined density of fresh water at temperature below $10°C$ if we consider $T_m = 3.98°C$, $\rho_m = 1.000 \times 10^3\ kg.m^{-3}$ and $\beta = 8.0 \times 10^{-3}\ kg.m^{-3}(°C)^{-2}$ [14, 15] and all other fluid properties (e.g. viscosity, thermal diffusivity) are assumed constant. We also assume that the flow is time dependent and two dimensional, and that the liquid property is constant except for the water density, which changes with temperature and in turn results to the buoyancy force. We can non-dimensionalise the coordinates x, y, velocity components u, v, time t, pressure p and temperature T by

$$U = \frac{u}{U_*} \quad V = \frac{v}{U_*} \quad X = \frac{x}{H} \quad Y = \frac{y}{H} \quad \tau = \frac{t}{\frac{H}{U_*}} \quad P = \frac{p}{\rho U_*^2}$$

$$\phi = \frac{T - T_\infty}{T_m - T_\infty}, \tag{2}$$

where x and u are horizontal, y and v are vertical; $U_* = \sqrt{\frac{\rho_\infty - \rho)}{\rho} H}$ is the relative frontal velocity and domain height H. We also define dimensionless parameters, the Reynolds Re, Prandtl Pr and Froude Fr numbers, by

$$\nu = \frac{\mu}{\rho} \quad \alpha = \frac{k}{\rho c_p} \quad Re = \frac{U_* H}{\nu} \quad Pr = \frac{\nu}{\alpha} \quad Fr^2 = \frac{\rho_m U_*^2}{g\beta(T_m - T_\infty)^2 H}, \tag{3}$$

where ν and α are the respective diffusivities of momentum and heat, and μ is viscosity, k is thermal conductivity and c_p is specific heat capacity. In terms of these dimensionless variables and parameters, the continuity equation, the horizontal and vertical momentum equations and the thermal energy equation are given as

$$\frac{\partial U}{\partial X} + \frac{\partial V}{\partial Y} = 0 \tag{4}$$

$$\frac{\partial U}{\partial \tau} + U\frac{\partial U}{\partial X} + V\frac{\partial U}{\partial Y} = -\frac{\partial P}{\partial X} + \frac{1}{Re}(\frac{\partial^2 U}{\partial X^2} + \frac{\partial^2 U}{\partial Y^2}) \tag{5}$$

$$\frac{\partial V}{\partial \tau} + U\frac{\partial V}{\partial X} + V\frac{\partial V}{\partial Y} = -\frac{\partial P}{\partial Y} + \frac{1}{Re}(\frac{\partial^2 V}{\partial X^2} + \frac{\partial^2 V}{\partial Y^2}) + \frac{1}{Fr^2}[\phi^2 - 2\phi] \tag{6}$$

$$\frac{\partial \phi}{\partial \tau} + U\frac{\partial \phi}{\partial X} + V\frac{\partial \phi}{\partial Y} = \frac{1}{RePr}(\frac{\partial^2 \phi}{\partial X^2} + \frac{\partial^2 \phi}{\partial Y^2}) \tag{7}$$

The terms U_{dc} and L_{dc} are used to describe the propagating speed and spread length of the density current. Our initial conditions are an undisturbed, homogeneous medium as also given in [2].

$$U = 0, \quad V = 0, \quad \phi = 0, \quad for \quad \tau < 0 \tag{8}$$

For $\tau \geq 0$ we have boundary conditions as follows. On the side walls:

$$U = 0, \quad V = 0, \quad \frac{\partial \phi}{\partial X} = 0 \tag{9}$$

At the plume source:

$$U = U_*, \quad V = 0, \quad \phi_{in} = 1 \text{ for } L/14 \text{ and } 0.07L/14 \text{ and } \phi_{in} = 0 \text{ for } 13L/14 \text{ and } 13.93L/14, \quad \text{for} \quad X = 0, \, at \; Y = H \tag{10}$$

On the floor of the domain:

$$U = 0, \quad V = 0, \quad \frac{\partial \phi}{\partial Y} = 0 \tag{11}$$

At the top of the domain:

$$\frac{\partial U}{\partial Y} = 0, \quad V = 0, \quad \frac{\partial \phi}{\partial Y} = 0 \tag{12}$$

The Reynolds number $Re = 50$, Froude number $Fr = 1$ and Prandtl number $Pr = 11$ will be fixed throughout this investigation. The dimensionless temperature $\phi_{in} = 1$ on $L/14$ and $0.07L/14$ is equivalent to a discharge at $4°C$ into an ambient at $0°C$. Numerical solution of the above equations is by means of COMSOL Multiphysics software. This commercial package uses a finite element solver with discretization by the Galerkin method and stabilisation to prevent spurious oscillations. We have used the "Extremely fine" setting for the mesh. Time stepping is by COMSOL's Backward Differentiation Formulas. Further information about the numerical methods is available from the COMSOL Multiphysics website [16]. Results will be illustrated mainly by surface temperature plots of dimensionless temperature on a colour scale from dark red for the ambient temperature $\phi = 0.0$, through yellow to white for the source temperature $\phi = 1$. Except at some point in the density current where we may have repeated temperature colour scale for a different temperature. Note that $\phi = 1.0$ corresponds to the temperature of maximum density.

3 Results and Discussion

The results here shows the behaviour of warm but dense fluid, discharged at $4°C$ through lock-exchange in cold fresh water. Reynolds number $Re = 50$, Froude number $Fr = 1$ and Prandtl number $Pr = 11$, are kept fixed throughout the study. Computational domain were also varied between $L = 7000$ and $L = 10000$ with barrier position between $L/14$ and $0.07L/14$ respectively. Figure 2, 3, 4, 5, 6, 7, 8 & 9 shows the evolution of temperature field for $\phi_{in} = 1$ within the time range $0 \leq \tau \leq 425$ and $0 \leq \tau \leq 1800$ in the various cases for a thorough analysis. Barrier position in the case as shown in Figure 2 is at $L/14$, with $\phi_{in} =$

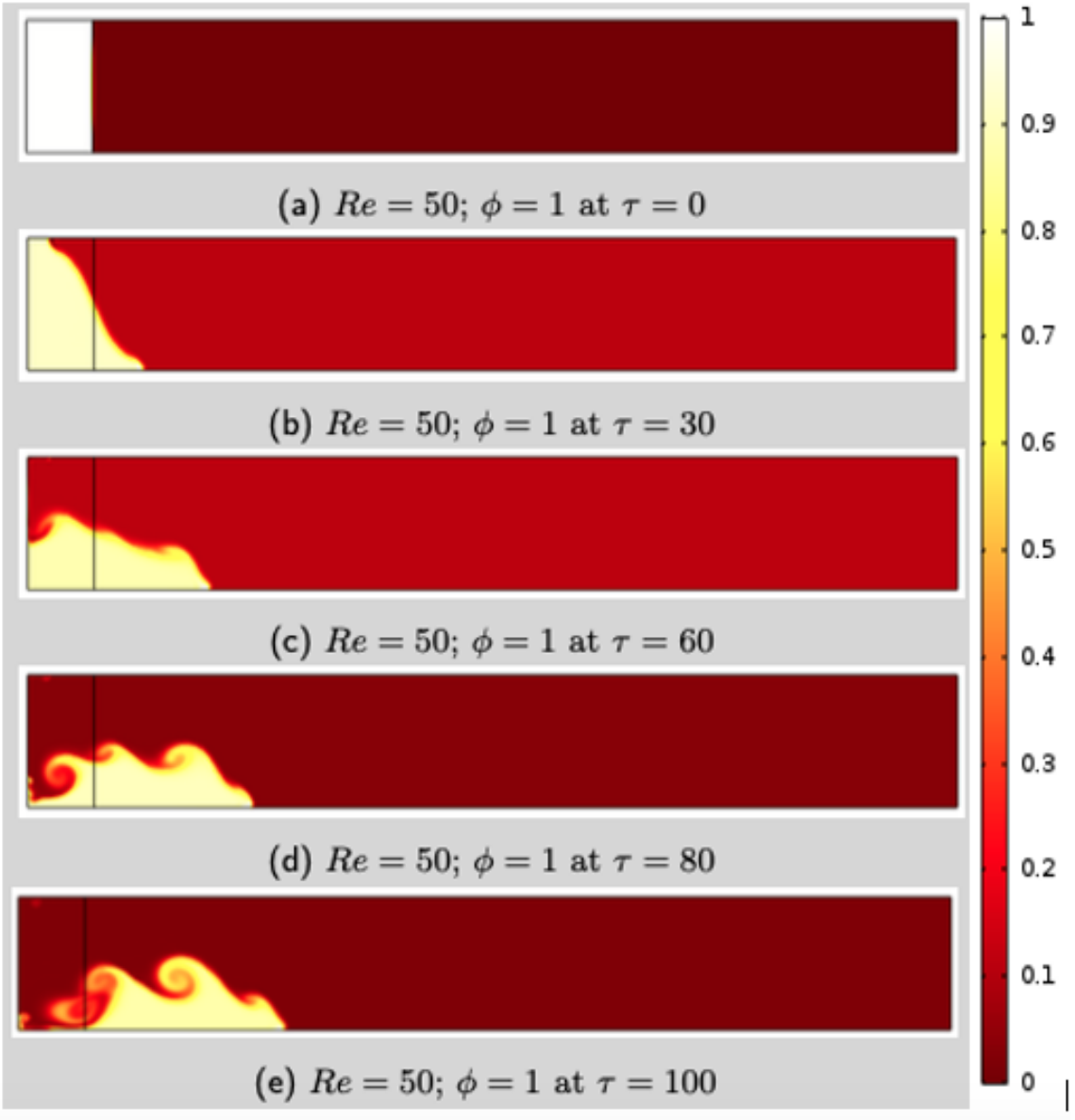

Fig. 2: Evolution of temperature field in the Density current for $Fr = 1$ and Reynolds number $Re = 50$ with $\phi = 1$ at time $0 \leq \tau \leq 100$

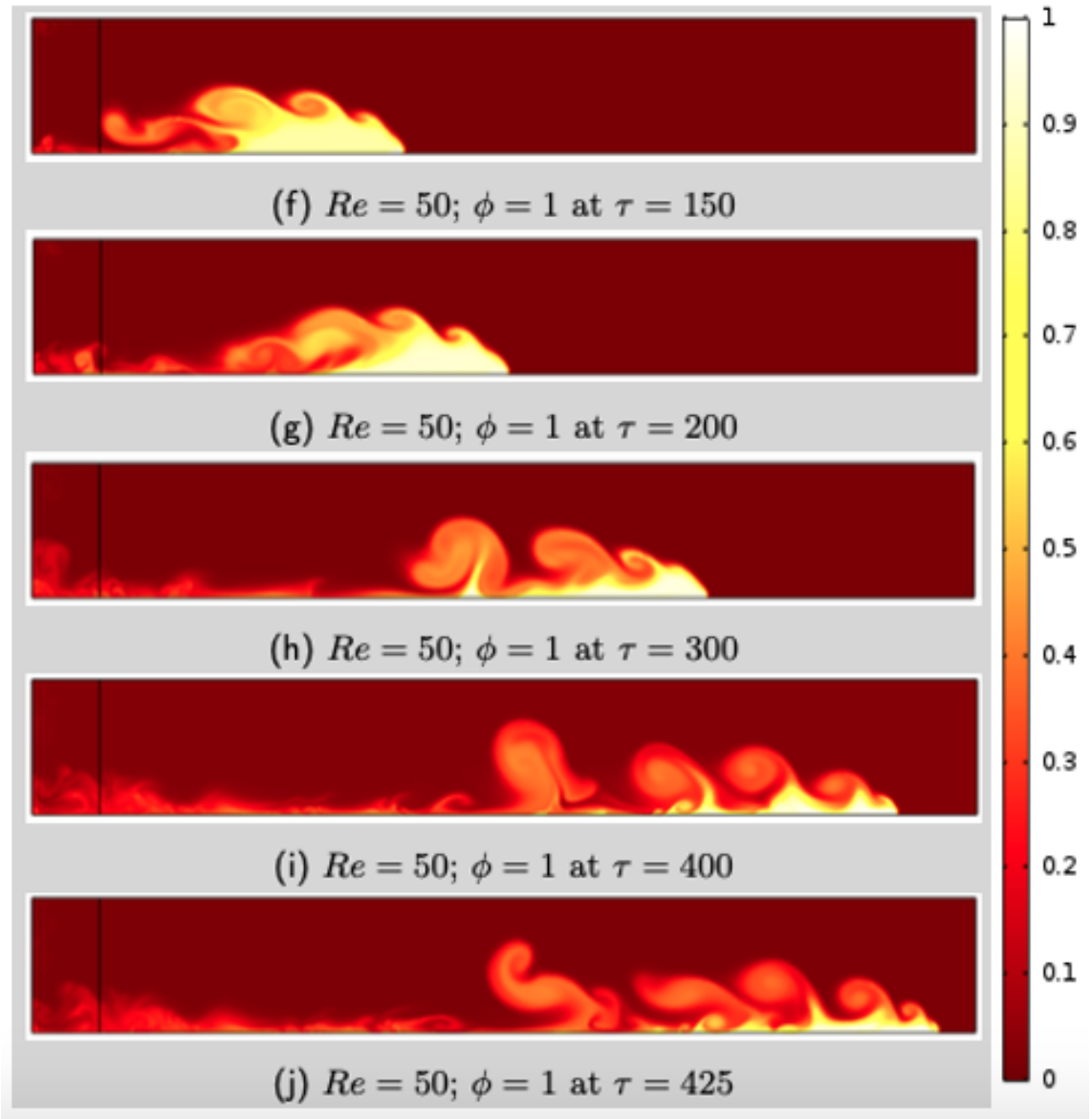

Fig. 3: Evolution of temperature field in the Density current for $Fr = 1$ and Reynolds number $Re = 50$ with $\phi = 1$ at time $150 \leq \tau \leq 425$

1 on the right hand side, and $\phi_{in} = 0$ on the left hand side. Meanwhile, that in the case as shown in Figure 4 is at $0.07L/14$, with $\phi_{in} = 1$ on the right hand side, and $\phi_{in} = 0$ on the left hand side.

A collapsing behaviour of the warm but denser fluid was observed within the first few time interval of the simulation, immediately after the removal of the barrier vertically upwards. A cabbeling process also begins within the same time at the point where the water masses meet, even as the denser fluid on the right hand side began to form density current (see Fig. 2(b) & 4(b)). A significant mixed fluid was not observed within this period and this might be as a result of the fact that the temperature difference between the two fluid is small. As time progresses, we observed the development of Kelvin-Helmholtz instabilities at the interaction layer between the ambient and the denser fluid. This unstable structures ranges from the penetrating head to the rear of the density current (see Fig. 2(c - e)); though, this is not obvious in Fig. 4(c - e) because of its reduced volume. However, the most dense fluid continue to penetrate the ambient fluid with a sharp frontal head.

Figure 4(d) - (e) shows a very different behaviour as compared to those in Figure 2(d) - (e). We observed in the former that the collapsing velocity of the denser fluid was high, higher than every fluid movement elsewhere. Thus, on getting the floor of the domain there was an intense (vigorous) mixing which had led to a major depletion in its temperature and this is evident afterwards as compared to the later (see Fig. 3(f) - (g) & 5(f) - (g)). This in turn resulted in a rapidly reduced motion because the dense but warm fluid is no longer energetic enough to advance quickly Fig. 5(f) - (g). However, the frontal motion of the head of this density current continue to spread further, penetrating the ambient fluid and maintaining the unstable layer even as this (Kelvin-Helmholtz instabilities) increases with time (see Fig. 3(h) - (j), Fig. 6 and Fig. 7). As the denser fluid advances, it was also observed that the frontal head is always found to be replenished by a ground flow of warm but dense unadulterated water from the rear, enabling the density current to push further (see Fig. 3(i) - (j)). Whereas, Figure 6, 7, 8 & 9 still contains some mildly warm fluid at the rear. This is as a result of the initial intense mixing after the lock release that have resulted to the denser fluid not being energetic to penetrate further. Thus, it takes much longer time to advance to the position of the frontal head.

During the flow, the motion of the density current decreases in a stepwise manner even as the Kelvin-Helmholtz instabilities dies out at the rear (see Fig. 3(i) - (j) & Fig. 9). The possible explanation to this behaviour might be that the raging columns of the Kelvin-Helmholtz instabilities causes a separation/partition in the denser fluid and after a given time interval, the most energetic dense fluid will regroup. This process will continue until the denser fluid will becomes the same temperature with the ambient fluid (see Fig. 3(h) - (j)). This is also the primary cause why the slightly warm fluid in Figure 6, 7, 8 & 9 is seen at the rear though, not energetic. The volume of dense but warm fluid reduces significantly as time progresses after the density current had moved a remarkable distance L_{dc} and as well as the propagation speed U_{dc} (almost to a halting state in this case with barrier position $0.07L/14$): and U_{dcc} (still energetic to penetrate further) as compared to the former, when measured from the barrier position. The density current will eventually halt as this becomes the same temperature with the ambient fluid Fig. 9.

With these information provided, we can clearly state that three phases or regimes of flow exist. First was the collapsing phase. This occur after the removal of the barrier, where water rapidly reorganised itself on the floor to advance forward. Second was the phase of rapid depletion of temperature because of the intense mixing after it landed, which resulted in a very slow motion because the temperature of the denser fluid at this point had reduced drastically, so it is not very energetic to accelerate faster. The third phase is the stepwise movement phase. This was the phase we observed much of the Kelvin-Helmholtz instabilities at the interaction layer. Where the raging columns of the Kelvin-Helmholtz instabilities causes a separation/partition in the denser fluid.

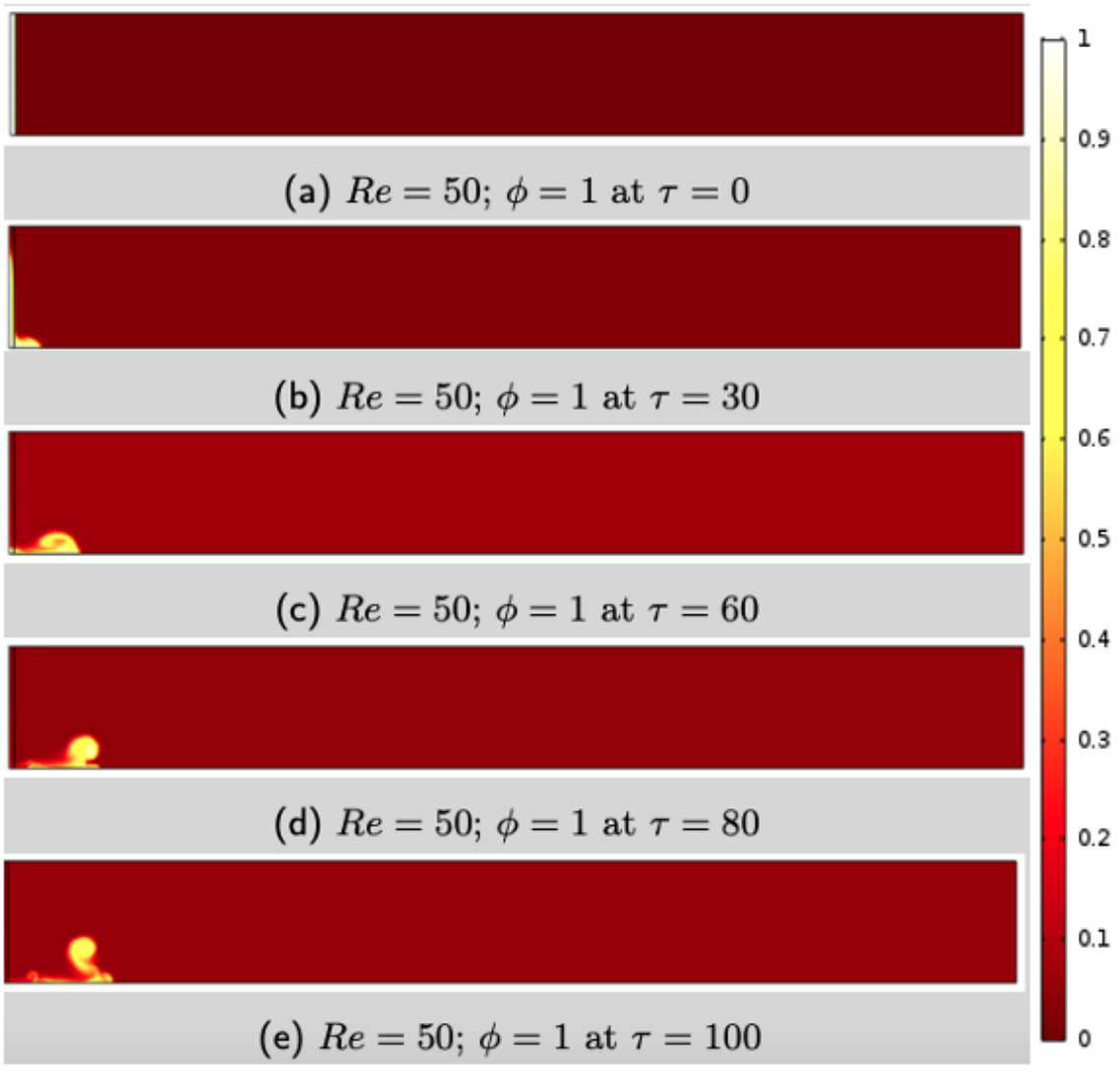

Fig. 4: Evolution of temperature field in the Density current for $Fr = 1$, $Pr = 11$ and $Re = 50$ with $\phi = 1$ at time $0 \leq \tau \leq 100$

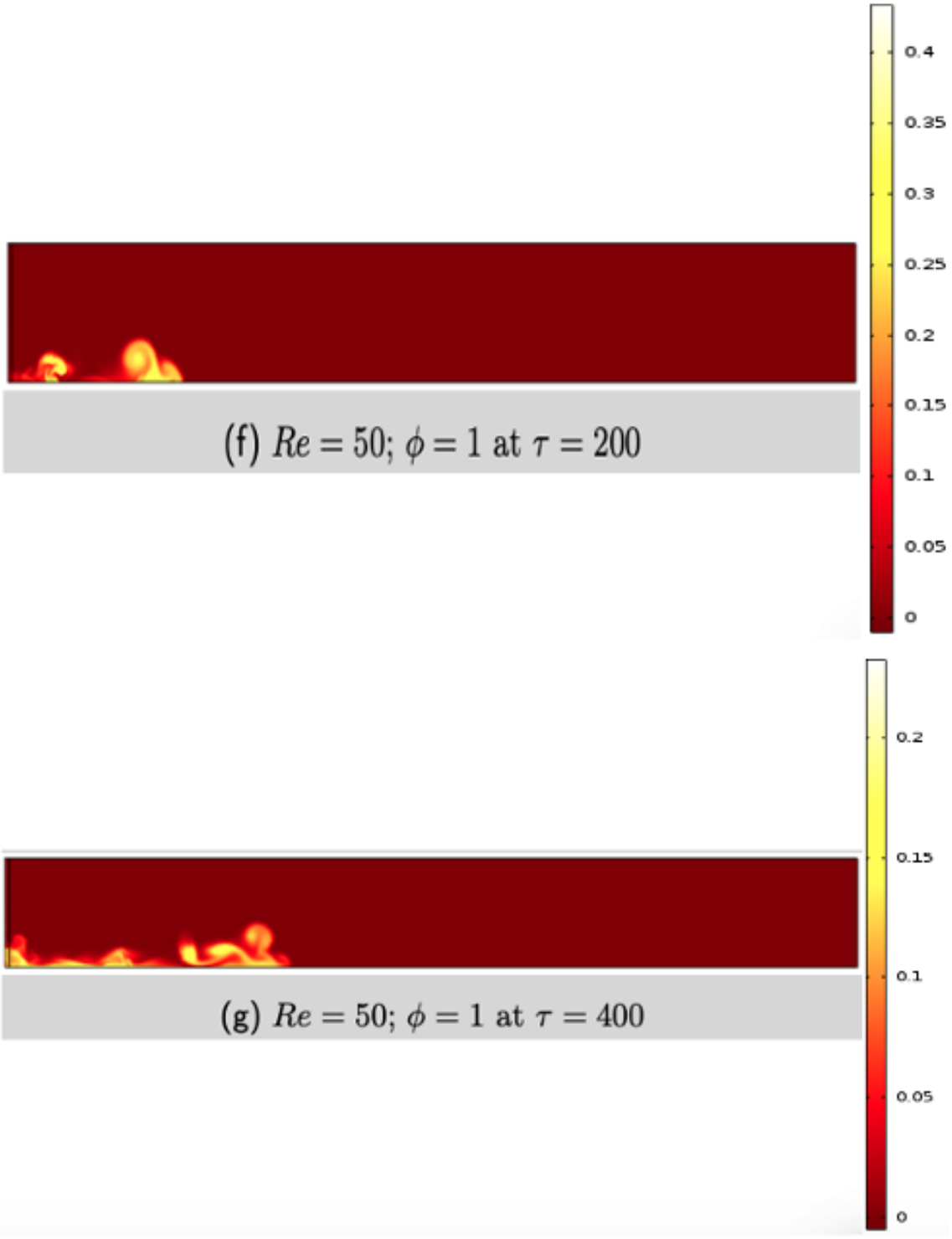

Fig. 5: Evolution of temperature field in the Density current for $Fr = 1$, $Pr = 11$ and $Re = 50$ with $\phi = 1$ at time $200 \leq \tau \leq 400$

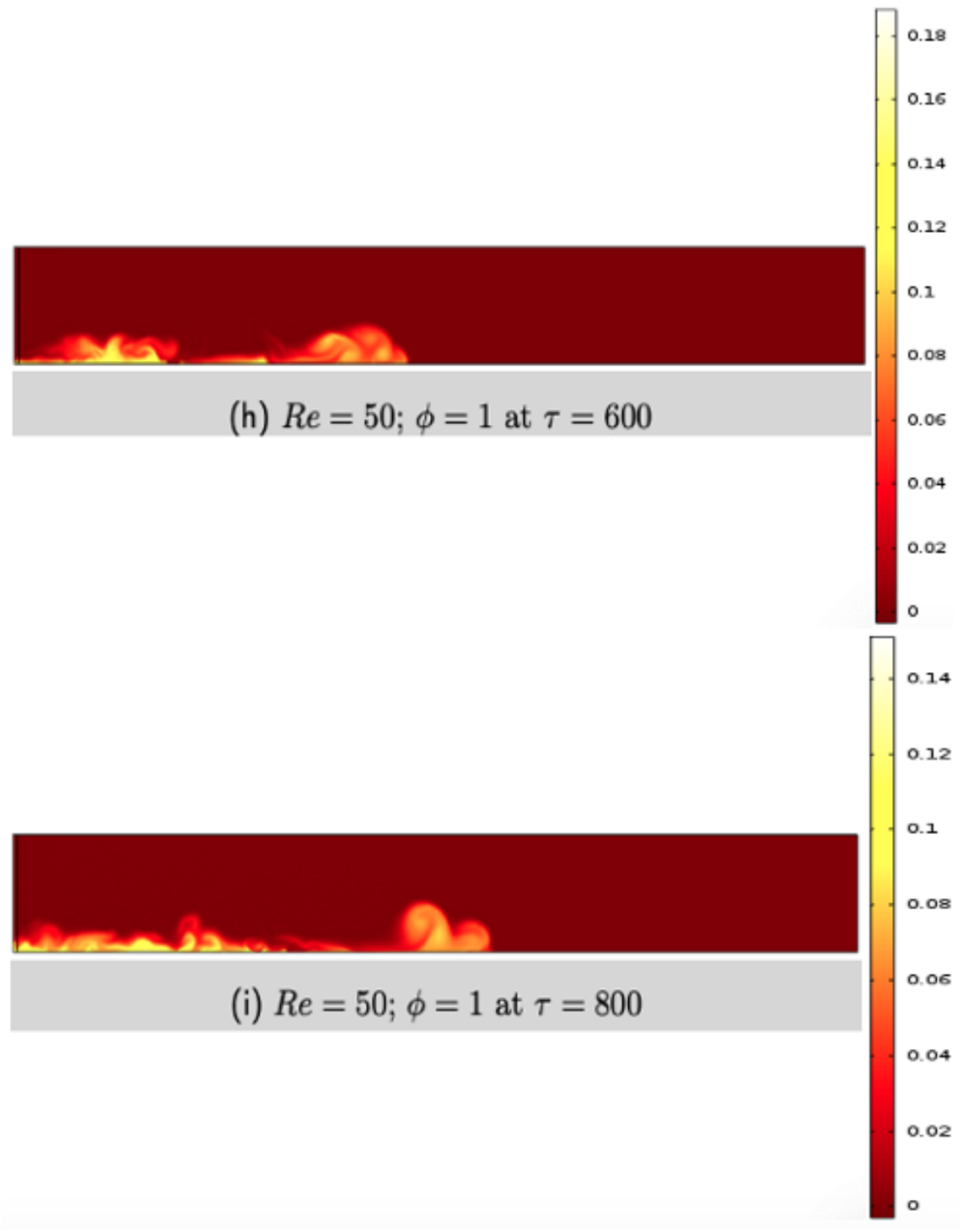

Fig. 6: Evolution of temperature field in the Density current for $Fr = 1$, $Pr = 11$ and $Re = 50$ with $\phi = 1$ at time $600 \leq \tau \leq 800$

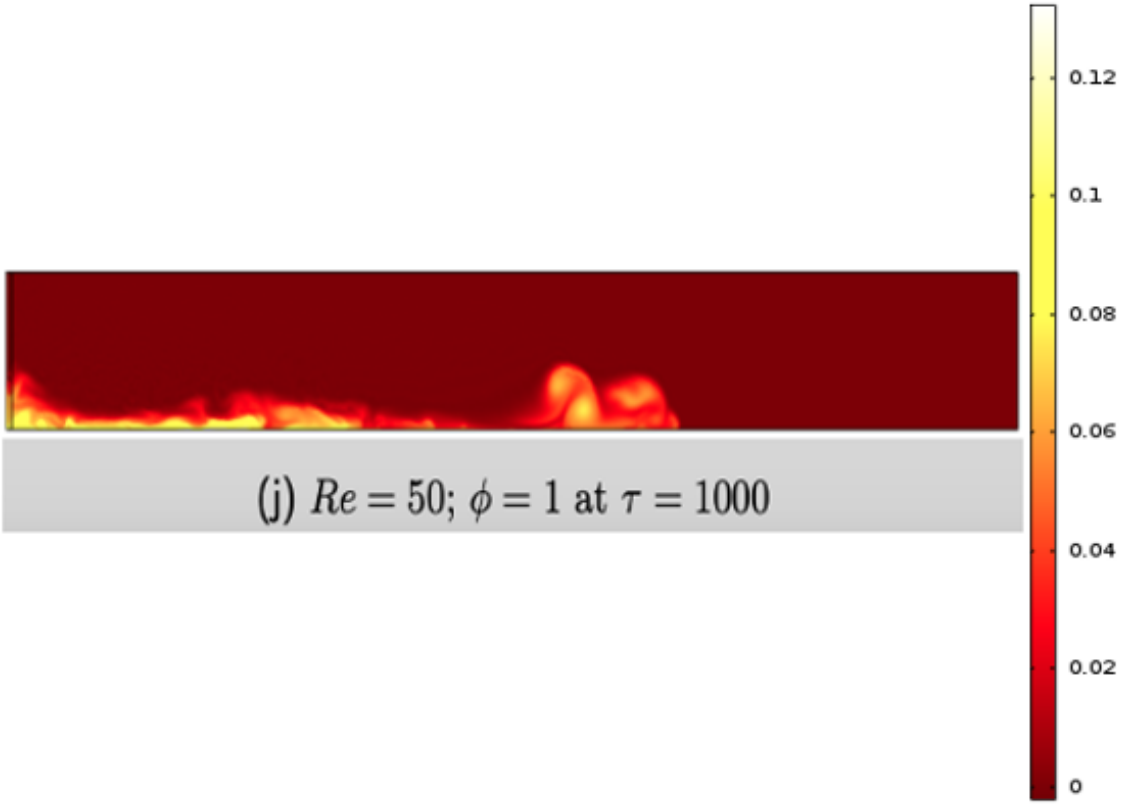

Fig. 7: Evolution of temperature field in the Density current for $Fr = 1$, $Pr = 11$ and $Re = 50$ with $\phi = 1$ at time 1000

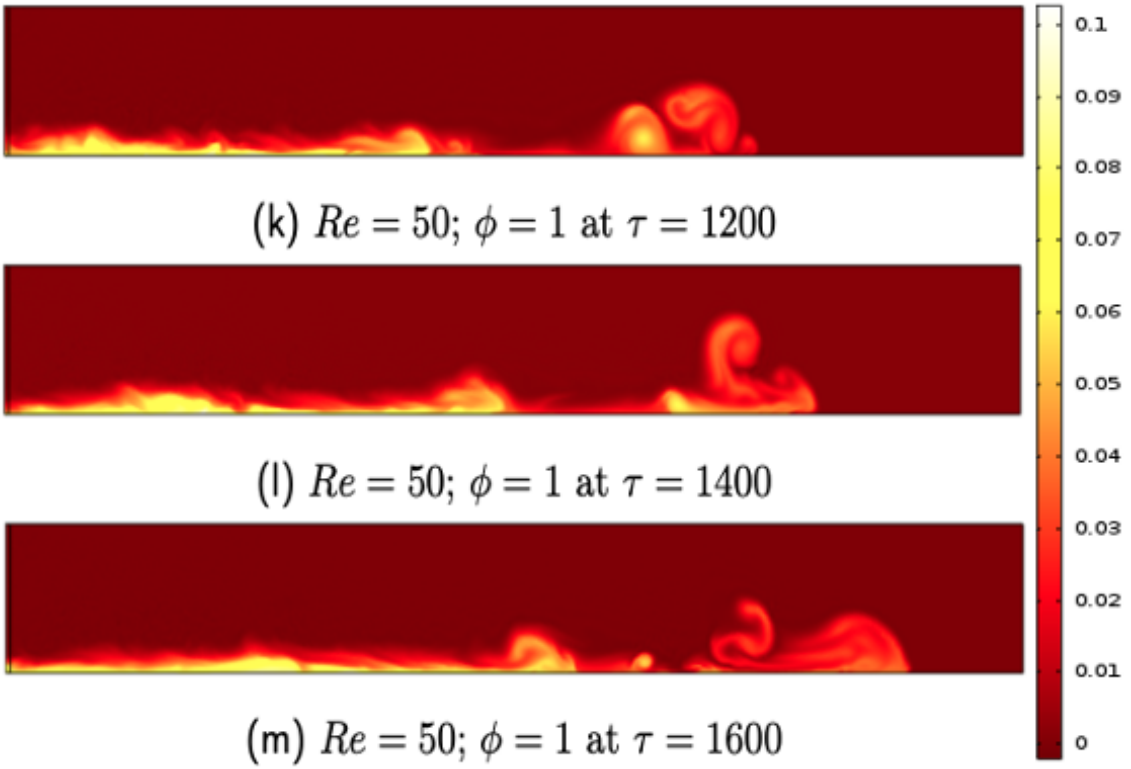

Fig. 8: Evolution of temperature field in the Density current for $Fr = 1$, $Pr = 11$ and $Re = 50$ with $\phi = 1$ at time $1200 \leq \tau \leq 1600$

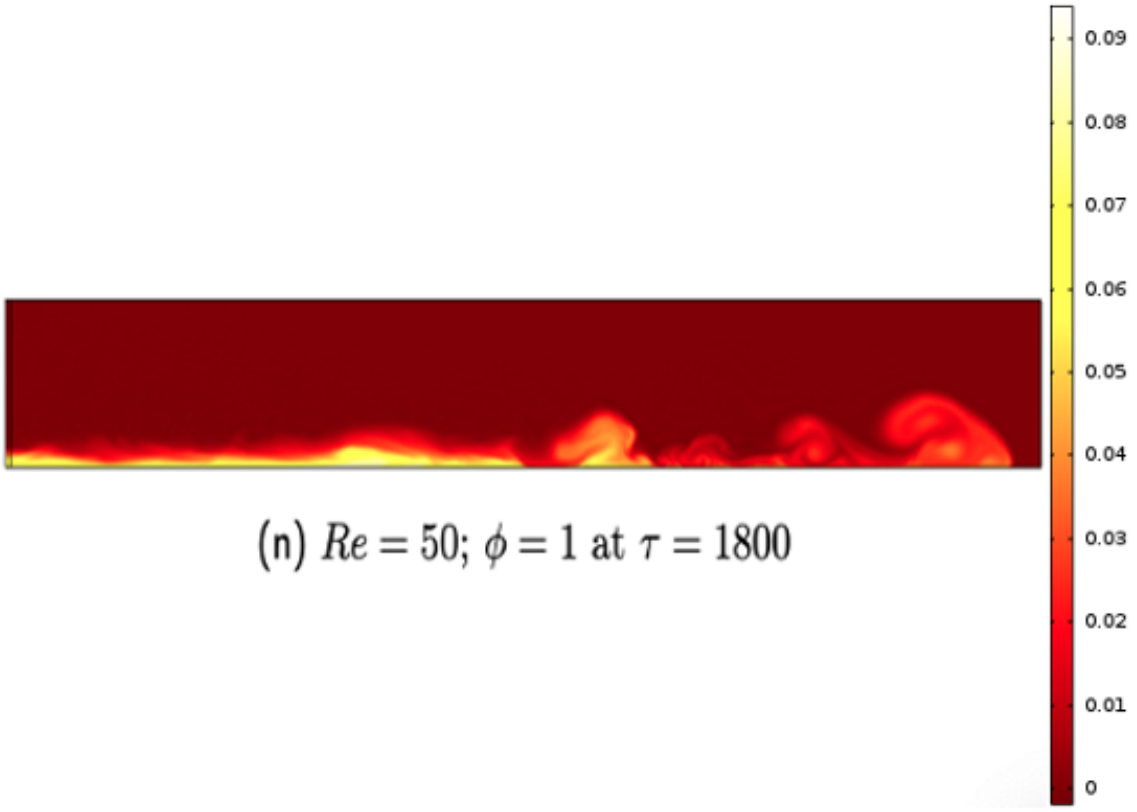

Fig. 9: Evolution of temperature field in the Density current for $Fr = 1$, $Pr = 11$ and $Re = 50$ with $\phi = 1$ at time 1800

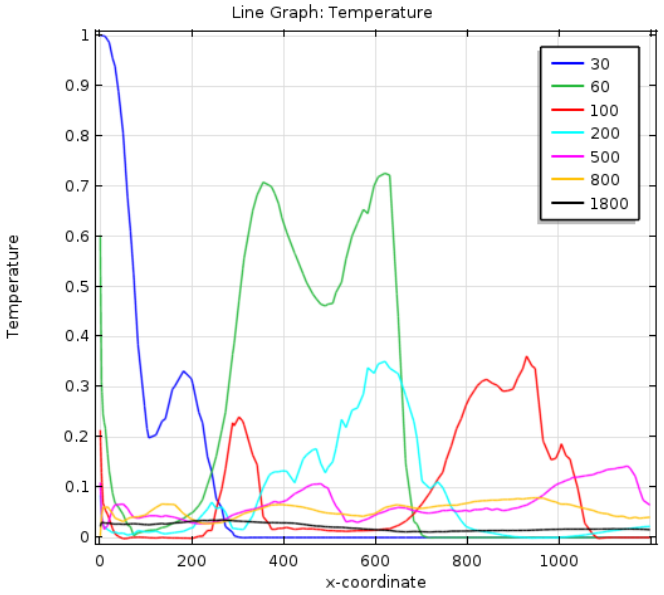

(a) $Re = 50$; $\phi = 1$ and $Pr = 11$

Fig. 10: Dimensionless temperature profiles at some point close to the floor of the domain $\phi(X, 100)$ at time $\tau = 30, 60, 100, 200, 500, 800, 1800$ in the Density current for $Re = 50$, $Pr = 11$, $\phi_{in} = 1$ and $Fr = 1$

We can now comfortably state that the various behaviours as observed here in this paper also corresponds to some of the earlier experimentally studied cases by Nogueira et al. [4], Adduce et al. [9] and Bukreev [13]. Noting that gravity currents usually undergo either two or three distinct phases of flow: a slumping phase, self-similar phase and viscous phase. That the instantaneous release of the two fluids after gate was removed led to an initial adjustment phase where the advancing head varies with approximately constant velocity. Though, we have also highlighted in the slumping phase that the collapsing velocity of the denser fluid within this time frame is high, higher than every fluid movement elsewhere. This behaviour is evident in Fig. 12(a) where there is a rapid linear movement. The second phase (self-similar phase) begins immediately after the ambient fluid reflected at the rear wall, this it in turn overtakes the penetrating head of the density current. In this phase our result shows a rapid depletion of temperature because of the intense mixing after the denser fluid landed, which resulted in a very slow motion because the temperature of the denser fluid at this point had reduced drastically, so it is not energetic enough to accelerate faster. The third phase is the phase where viscous effects overcome inertial effects and the current front velocity decreases more rapidly as $t^{-\frac{4}{5}}$ as also sited in [2]. In this present study, our result shows a stepwise movement. This was the phase we observed much of the Kelvin-Helmholtz instabilities at the interaction layer. Where the raging columns of the Kelvin-Helmholtz instabilities causes a partition in the denser fluid, which might be responsible for the stepwise movement. Note that the previous experimentally studied cases that the initial density difference is usually by adding salt to the fluid on either side of the barrier, so as to produce a denser fluid [4, 9] . Except for Bukreev [13] who considered density variation is as a result of temperature difference, but did not really give much details.

Profiles of temperature and horizontal velocity component on the density current at the height $Y = 100$ at some distance above the floor were also examined. This enables us to gain more information on the

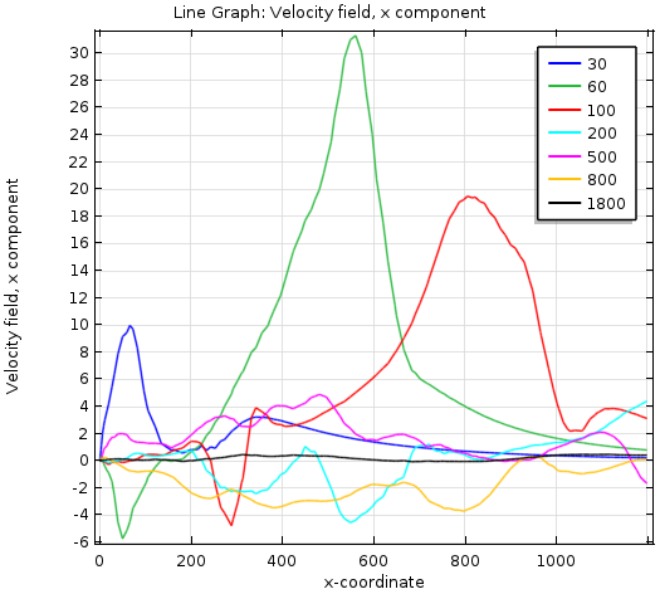

(a) $Re = 50$; $\phi = 1$ and $Pr = 11$

Fig. 11: Dimensionless horizontal velocity profiles at some point close to the surface $V(X, 100)$ at time $\tau = 30, 60, 100, 200, 500, 800, 1800$ in the Density current for $Re = 50$, $Pr = 11$, $\phi_{in} = 1$ and $Fr = 1$

spreading behaviour of the density current for effective analysis as shown in Figure10 and Figure.11. The Profiles of temperature (Fig.10) shows that there was a serious depletion of temperature within the first few interval between $L = 0 - 200$, except at $\tau = 30$ where we could still observe a fairly warm fluid within the range. At time $\tau = 60$, within the interval $L = 200 - 600$, we could trace fairly undiluted denser fluid. This we also believed to be true because the development of Kelvin-Helmholtz instabilities is yet to begin at that point in time. Thereafter, there was intense mixing also resulting from the Kelvin-Helmholtz instabilities leading to further depletion of temperature downstream. Most of the fluid within the time range $500 \leq \tau \leq 1800$ at that level was already at the same temperature with the ambient fluid. Thus, we can conclude that, temperature decreases rapidly with time at that level. With discharge temperature $\phi = 1$, the density current just required little mixing to attain the same density as that of the ambient. The development of Kelvin-Helmholtz instability as it penetrates further enables the denser water to blind very fast with the ambient. And in fact, fluctuations in the temperature profiles also confirm that decrease in temperature with horizontal length is not monotonic. In like manner, profiles of horizontal velocity (Fig.11) shows that there was some level of backward and forward movement of the fluid at that level. The possible explanation to this might be as a result of the interaction layer between the two fluid, where Kelvin-Helmholtz instabilities was observed. As the frontal head pushes forward, the mixed fluid that is up $\phi = 0$ moves to the rear with the aid of the Kelvin-Helmholtz instabilities. Though, a very fast forward movement of the fluid is evident at some point $X = 500\, and\, 800$. It is worth indicating that both profiles of temperature and that of velocity are determined from the simulation as shown in Figure 9.

The propagation speed with which the frontal head of the density current U_{dc} travels with time τ_n is also presented and shown with a linear and logarithmic scale in Figure 12(a) for simulations with barrier point $0.07L/14$. As described earlier, our results here had shown three phases or regimes of flow. First was the

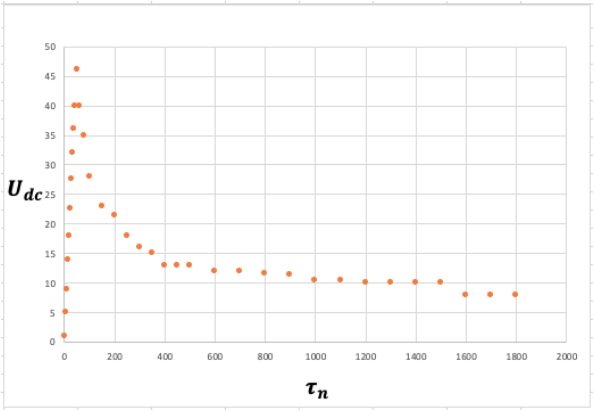

(a) Linear Scale

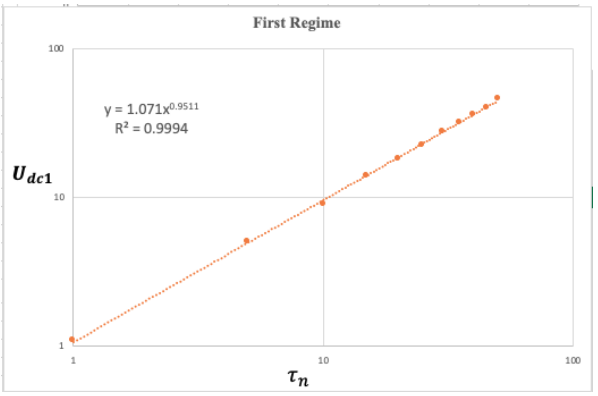

(b) Logarithmic Scale

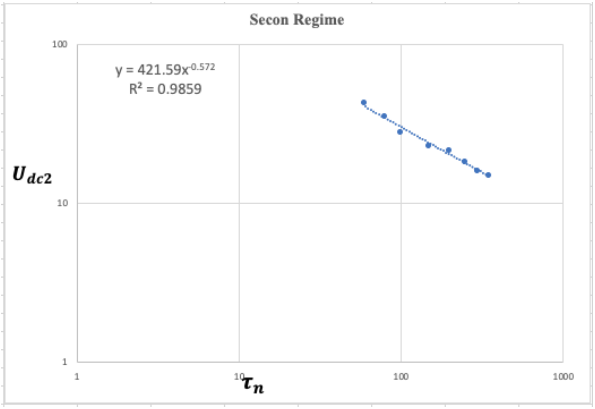

(c) Logarithmic Scale

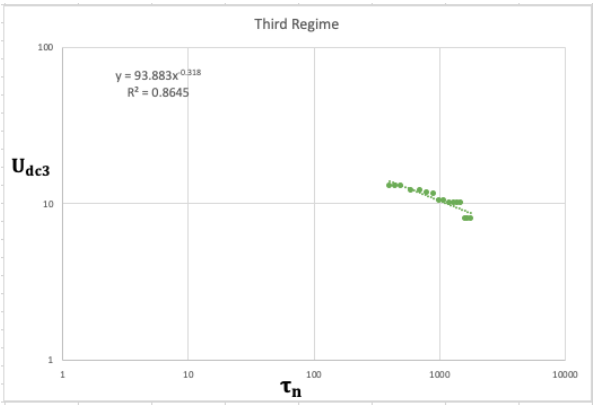

(d) Logarithmic Scale

Fig. 12: Propagation speed of the Density current U_{dc} for the different Regimes with respect to time τ_n.

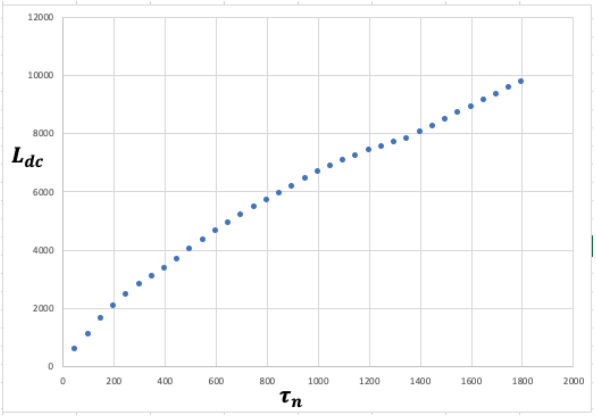

(a) Linear Scale

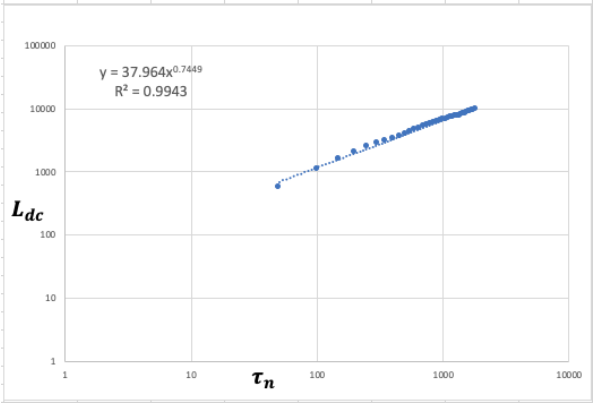

(b) Logarithmic Scale

Fig. 13: Variation of spreading distance of the density current L_{dc} with respect to time τ_n.

collapsing phase which correspond to the description as given in [12, 13] (slumping phase). This occurs after the removal of the barrier, where water rapidly reorganised itself on the floor to advance forward. However, we have recorded the case that the collapsing velocity of the denser fluid within this time frame is high, higher than every fluid movement elsewhere. This behaviour is evident in Fig. 12(b) where there is a rapid linear movement. Therefore, we can identify a single regime in this phase of flow from an empirically determined data set, and this is shown as a straight line that represents the best fit power laws obtained by linear regression of $logU_{dc1}$ on $log\tau_n$:

$$U_{dc1} = 1.071\tau_n^{0.9511} \quad [R^2 = 0.9994] \tag{13}$$

where R^2 is the regression coefficient in each case.

Second was the phase of rapid depletion of temperature because of the intense mixing during the reorganising process on the floor. This we can liken to as the self-similar phase where after the ambient fluid had reflected at the rear wall it in turn overtakes the penetrating head of the current. It was reported earlier that at this point in the flow, the penetrating head advances as $t^{\frac{2}{3}}$, but decreases with front speed as $t^{-\frac{1}{3}}$ [4]. However, our results here shows slightly different in terms of the scaling laws. In our case here, based on the rapid depletion of temperature resulting from the intense mixing as dense fluid try to reorganise itself on the floor. This process resulted in a very slow movement of the fluid, because the temperature of the denser fluid at this point had reduced drastically, and not energetic to accelerate faster (see Fig. 12(c)) where we observe a downward slop. Therefore, we can identify a single regime in this phase of flow from an empirically determined data set, and this is shown as a fairly straight line that represents the best fit power laws obtained by linear regression of $logU_{dc2}$ on $log\tau_n$:

$$U_{dc2} = 421.59\tau_n^{-0.572} \quad [R^2 = 0.9859] \tag{14}$$

where R^2 is the regression coefficient in each case.

The third phase is the stepwise movement phase which corresponds to the phase where viscous effects overcome inertial effects and the current front velocity decreases more rapidly as $t^{-\frac{4}{5}}$, with front position advancing as $t^{\frac{1}{5}}$ [4]. Whereas, our results also shows a very unique behaviour here. This was the region where much of the Kelvin-Helmholtz instabilities at the interaction layer was observed. Such that the raging columns of the Kelvin-Helmholtz instabilities causes a partition in the denser fluid which might be responsible for the stepwise movement. However, we could identify a single regime in this phase of flow from an empirically determined data set, and this is shown in Figure 12(d) as a fairly straight line that represents the best fit power laws obtained by linear regression of $logU_{dc3}$ on $log\tau_n$:

$$U_{dc3} = 93.883\tau_n^{-0.318} \quad [R^2 = 0.8645] \tag{15}$$

where R^2 is the regression coefficient in each case.
The results as presented here (see Fig. 12(a)) with a linear scale are similar to the experimentally studied cases by Bukreev [13] and [17], where the author have considered the speed of the surface current at different barrier position.

Spreading distance L_{dc} of the density current were also considered with a linear and logarithmic scale (see Fig. 13(a) and (b)). These data are empirically determined spread length L_{dc} of the density current, measured from the barrier position to a significant distance and plotted against time τ_n. Both results with the linear and logarithmic scale (Fig. 13(a)) shows that a single regime could be identified, shown as a straight line that represents the best fit power laws obtained by linear regression of $logL_{dc}$ on $log\tau_n$:

$$L_{dc} = 37.964\tau_n^{0.7449} \quad [R^2 = 0.9943] \tag{16}$$

4 Conclusion

Thorough investigation had been carried out on the behaviour of warm discharge through lock exchange, with the assumption that density was taken as a quadratic function of temperature. The results here shows some level of similarities to those experimentally cases by Nogueira et al. [4], Adduce et al. [9] and Bukreev [13], where the development of Kelvin-Helmholtz instability was observed after some time interval in the density current. We were able to observe the distinct three phases of flow in the present investigations, a collapsing (slumping) phase, self-similar phase and viscous phase as described in earlier studies [2, 4,9] and this became obvious when considering the speed U_{dc} with which the density current travels with respect to time. However, we were able to observe in the slumping phase that the collapsing velocity of the denser fluid within this time frame is high, higher than every fluid movement elsewhere. This shows a rapid linear movement. A vigorous mixing was also observed immediately after the collapsing phase that led to a rapid depletion of temperature resulting to a very slow motion as denser fluid was not energetic enough to accelerate faster. Our result also shows a stepwise movement and this we believe might be as much of the Kelvin-Helmholtz instabilities at the interaction layer was developed where the raging columns of the Kelvin-Helmholtz instabilities causes a partition in the density current. The previous experimental cases by Nogueira et al. [4], Adduce et al. [9] had it that the initial density difference is usually by adding salt to the fluid on either side of the barrier. While Bukreev [13] considered density variation as a result of temperature difference, but did not obtain a relation that describe the rate of spread of the density current. Whereas, we were able to provide relations that describes the various regimes of flows as given in equation (13), (14) and (15). Relations were also drawn that describes the spreading distance L_{dc} of the density current and this is given in equation (16). Density current cases are practical cases that are evident in nature and human interventions. However, we are believing that the little variations in the scaling laws as compared to those by Nogueira et al. [4] and Huppert & Simpson [12] might be as a result of the fact that the present investigation had considered density variation as a result of temperature difference, while theirs was by adding salt to the fluid on either side of the barrier. Lastly, is the consideration of the barrier position. We also believe that the volume of denser fluid released into the ambient might also be a factor. Thus, there is the need to carryout a thorough investigation to fathom, if the speed of the current is dependent on the barrier position. This work as presented here is practical and relevant to many fields of study and also enhances policy making towards the protection of the aquatic ecosystems. Because such discharge or introduction of warm but dense water may definitely give rise to environmental problems; where the sudden increase in the water temperature after discharge/introduction will leads to "hermal shock" killing aquatic life that has become acclimatised to living in a stable temperate environment. Researchers can also gain more knowledge in terms of the dynamics of such flows.

References

[1] Simpson, J. E. (1997) *Gravity Currents: In the Environment and the Laboratory.* UK, Cambridge University Press, 258 pp.

[2] George, M. A. and Kay, A. (2022). Numerical Simulations of the Cabbeling Phenomenon in Surface Gravity Currents in Cold Fresh Water *Journal of Scientific Research & Reports* **28** *1* Pp. 68 - 85.

[3] Huppert, H. E. (1986). *The intrusion of fluid mechanics into geology. Journal of Fluid Mechanics,* **173,** Pp. 557.

[4] Nogueira, I. S. H., Adduce, C., Alves, E. and France, J. M. (2013). *Analysis of Lock-exchange gravity currents over smooth and rough beds. Journal of Hydraulic Research,* **51** *4* Pp. 417 - 531.

[5] Ooi, K. S., Constantinescu, G. and Weber, L. (2009). *Numerical simulations of lock-exchange compositional gravity current. Journal of Fluid Mechanics,* **635,** Pp. 361 - 388.

[6] Prandtl, L. (1952) *Essentials of fluid dynamics.* UK, Blackie & Son

[7] Benjamin, T. B. (1986). *Gravity currents and related phenomena. Journal of Fluid Mechanics,* **31,** *2* Pp. 209 - 248.

[8] Rottman, J. W., and Simpson, J. E. (1983). *Gravity currents produced by instantaneous releases of a heavy fluid in a rectangular channel. Journal of Fluid Mechanics,* **135,** Pp. 95 - 110.

[9] Adduce, C., Sciortino, G. and Proietti, S. (2012). *Gravity Currents Produced by Lock Exchanges: Experiments and Simulations with a Two-Layer Shallow-Water Model with Entrainment. Journal of Hydraulic Engineering,* **138,** *2* Pp. 111 - 121.

[10] Nogueira, I. S. H., Adduce, C., Alves, E. and Franca, J. M. (2013). *Image analysis technique applied to lock-exchange gravity currents. Meas. Sci. Technol.,* **24** Pp. 1 - 4.

[11] Cenedese, C., Nokes, R and Hyatt, J. (2016). *Lock-exchange Gravity Currents over Rough Bottoms Journals of Environmental Fluid Mechanics* doi:10.1007/s10652-016-9501-0

[12] Huppert, H. E. and Simpson, J. E (1980). *The Slumping of Gravity Currents. Journal of Fluid Mechanics* **99** Pp. 785 - 799.

[13] Bukreev, I. V. (2006). *Effect of the Nonmonotonic Temperature Dependence of Water Density on the Decay of an initial Discontinuity. Journal of Applied Mechanics and Technical Physics,* **47** *1* Pp. 54 - 60.

[14] Moore, D. R. and Weiss, N. O. (1973). Nonlinear penetrative convection. *Journal of Fluid Mechanics,* **61** Pp. 553 - 581.

[15] Oosthuizen, P. H. and Paul, J. T. (1996). A Numerical study of the Steady State Freezing of Water in an open Rectangular Cavity. *International Journal of Numerical Methods for Heat and Fluid Flow,* **6** *(5)*, Pp. 3-16

[16] COMSOL Multiphysics Cyclopedia. *The Finite Element Method (FEM). [ONLINE] Available at: https://www.comsol.com/multiphysics/finite-element-method [Accessed 28 April 2016].*

[17] Bukreev, I. V. (2006). *Effect of the Nonmonotonic Temperature Dependence of Water Density on the Propagation of a Vertical Plante Jet. Journal of Applied Mechanics and Technical Physics,* **47** *2* Pp. 169 - 174.